

## Direct Observation of an Increase in Buckled Dimers on Si(001) at Low Temperature

Robert A. Wolkow

*AT&T Bell Laboratories, Murray Hill, New Jersey 07974*

(Received 10 June 1991)

The first low-temperature scanning-tunneling-microscope (STM) images of Si(001) are presented. It is observed that on cooling to 120 K the number of buckled dimers increases, confirming that dimers have an asymmetric character. Buckled-dimer domains of  $c(4\times 2)$  order are bounded by  $p(2\times 2)$  regions. Defects pin nearby dimers into a buckled configuration and act to smear out the transition to order. At room temperature dimers rapidly switch orientation leading to an averaged symmetric appearance in STM images.

PACS numbers: 68.35.Bs, 61.16.Di, 68.35.Dv

The microscopic structure of the Si(001) surface was first probed over 30 years ago in a low-energy electron diffraction study (LEED) by Schlier and Farnsworth [1]. Evidence of a  $2\times 1$  structure was observed and a reconstruction based on the formation of dimers was proposed. Subsequent investigations revealed higher-order diffraction spots, of an intensity and sharpness that was highly dependent on sample treatment [2-4]. Theoretical modeling [5,6] together with photoemission [7] and LEED [8] analyses eventually established the surface dimer as the principal feature of the reconstructed Si(001) surface but the origin of higher-order diffraction spots remained controversial. It was recognized that buckled (i.e., tilted) dimers could account for higher-order diffraction. In addition, buckled dimers are consistent with the expectation that symmetric dimers should be subject to a Peierls distortion. In an empirical tight-binding calculation, Chadi predicted that symmetric dimers were unstable with respect to buckled dimers [9]. Chadi's results in turn led to further experimental effort. Ion scattering measurements were suggestive of buckling [10-12]. Complex dynamical LEED analyses were performed but did not yield compelling evidence of buckled dimers [13-15]. While the scanning-tunneling-microscopy (STM) measurements of Tromp, Hamers, and Demuth provided striking confirmation of surface dimers, the observation of both symmetric and buckled dimers fueled the controversy involving the dimer configuration [16]. A recent calculation incorporating spin effects led to the conclusion that symmetric dimers are most stable [17]. New high resolution photoemission data, on the other hand, indicate two inequivalent types of surface silicon atoms which are interpreted to be the up and down atoms of buckled dimers [18]. Pseudopotential calculations by Pandey [19], Payne *et al.* [20], and Roberts and Needs [21] show that the difference in energy between buckled and symmetric dimers is very small, near the limits of computational accuracy.

In this work we resolve the long-standing problem regarding the dimer configuration. A new variable-temperature STM is used to record the first low-temperature images of Si(001). We observe that on cooling to 120 K, the number of buckled dimers increases, at the expense of

symmetric appearing dimers, and it is concluded that dimers must have an innate bistable asymmetric character to account for the observed temperature dependence.

The experiments were performed with a unique variable-temperature STM which operates over the range 100 to 400 K, in ultrahigh vacuum. This instrument is described in detail elsewhere [22]. The entire STM including sample and tip are held isothermal and the instrument is temperature stabilized in 1 to 2 h. A given temperature can be maintained for more than 10 h. Tungsten tips were electrochemically etched in a NaOH solution and heated in vacuum before use. The crystals studied were *n*-type, 1 m $\Omega$  cm, Si(001) aligned with  $\frac{1}{2}^\circ$ . Crystal cleaning involved resistive heating at 680°C for 4 h, followed by several seconds at 1000°C. Samples cleaned in this way typically contain 5% to 10% surface defects. The pressure in the vacuum chamber is typically  $10^{-10}$  Torr or lower.

Figure 1 shows a room-temperature STM image of the Si(001) surface showing symmetric dimers, buckled dimers, and numerous defects. As has been previously reported [16], we note that buckled dimers occur only in the vicinity of defects or step edges. Dimers are evidently coupled within a row causing the influence of a defect to be transmitted along a row in an anticorrelated manner. Coupling of dimers results, at least in part, from lattice strain. This is shown schematically in the inset of Fig. 1. As the two second layer atoms bound to the up end of a dimer are drawn together, those bound to the down end are pushed apart. Adjacent dimers best accommodate this strain by buckling in the opposite sense.

The various defects present on the Si(100) surface may be broadly divided into two categories; those which induce buckling in adjacent dimers, and those that do not. In general, defects which induce buckling are themselves asymmetric in appearance, while those that do not induce buckling reveal no asymmetric structure. Examples of nonbuckling defects are indicated at *H* and *I* in Fig. 1. Examples of the most common type of buckle inducing defects are labeled *A*, *B*, and *C* in Fig. 1. This defect type appears to be identical to that identified previously by Hamers and Kohler [23], and has the appearance of two adjacent dimers, buckled in the same direction. The

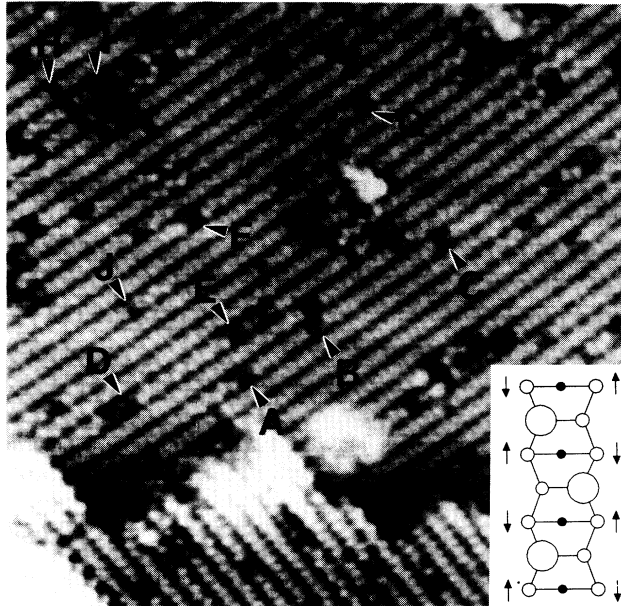


FIG. 1.  $240 \times 240 \text{ \AA}$  room-temperature constant-current topograph of Si(001) taken at  $-2 \text{ V}$  sample bias and  $0.3 \text{ nA}$ . Inset: A simple schematic view of the lattice strain which acts to couple adjacent dimers in an anticorrelated manner.

actual structure, and whether or not impurities are involved, is unknown. What is clear, however, is that defects of this type induce buckling such that adjacent dimers are tilted in the opposite sense to the defect itself. The magnitude and range of buckling near a defect is variable. Close inspection of Fig. 1 reveals that the effect of a particular defect is strongly modified by other nearby defects. For example, defect *A* shows buckling to the left but very little to the right. Defect *B* is 7 dimers removed and of the opposite type, resulting in a conflicting influence and little apparent buckling. Defects *B* and *C* also exert an out-of-phase influence on intervening dimers. However, the 14 dimer separation of defects is sufficient to allow 3 or 4 dimers adjacent to the defects to buckle. Buckling to the left of defect *A* and to the right of defect *C* is relatively unimpeded and extends 6 to 8 dimers. The in-phase influence of defects is also apparent. Defects *D* and *E* have 11 intervening dimers, all of which are buckled. Defects *F* and *G* also exert an in-phase influence, but are sufficiently well separated that dimers in the center of this section are not substantially buckled. In addition to in-row coupling, coupling between rows is also evident. Defect *E*, for example, induces buckling in the row above it at a point where the influence of in-row defects has clearly faded. In addition to the double buckled type defect, a variety of other buckle inducing defects is apparent. Defect *J* is particularly interesting as it is relatively isolated from the influence of other defects and yet displays stronger buckling to the right than to the left.

Figure 2 is a constant-current topograph of the Si(001) surface recorded at 120 K. The defect density on this

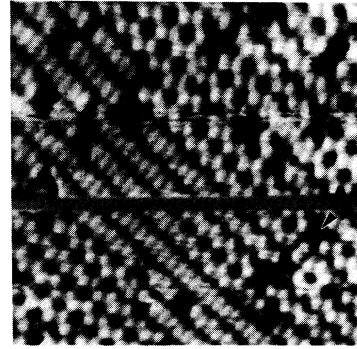


FIG. 2.  $110 \times 110 \text{ \AA}$  topograph of Si(001) taken at a temperature of 120 K at  $-2 \text{ V}$  sample bias and  $0.4 \text{ nA}$ . (The horizontal band resulted from an equipment malfunction during acquisition.)

surface is approximately 8% and is unchanged from room temperature. In sharp contrast to room-temperature images, extended regions of buckled dimers are clearly evident. In most cases buckling continues along a row with no apparent decay in magnitude. The row containing the defect labeled *A*, for example, shows 27 buckled dimers running from the defect to the edge of the image. Defect *A* is identical to the double buckled defects seen in the room-temperature image. Adjacent buckled rows can interact in two ways. The more common  $c(4 \times 2)$  arrangement results when the zigzag pattern of buckled rows is out of phase. The in-phase  $p(2 \times 2)$  arrangement is also present and can be seen, for example, in the lower right corner of the image. Given that defects are randomly scattered on the surface, it might be expected that adjacent buckled rows would take on  $p(2 \times 2)$  order as often as  $c(4 \times 2)$ . Since at low temperature  $c(4 \times 2)$  dominates, we conclude that row-row coupling, with a preference for  $c(4 \times 2)$ , plays a significant role in forming extended two-dimensional ordered domains. It is likely that dimer rows containing defects which do not include buckling follow the influence of adjacent buckled rows. In addition to ordered regions, symmetric appearing dimers, and buckling which decays with distance from a defect, are also present at 120 K.

A larger area of the surface at 120 K is shown in Fig. 3. Individual dimers are not resolved but the zigzag pattern of buckled-dimer rows stands out clearly enough in most cases, particularly so in  $c(4 \times 2)$  regions which have a honeycomb appearance. We find that over 80% of the surface is buckled and that  $c(4 \times 2)$  ordering between rows is more than 5 times more common than  $p(2 \times 2)$ . (Figure 2 shows a greater proportion of symmetric dimers than is typical.) The image on the right-hand side of Fig. 3 has  $c(4 \times 2)$  domains outlined. Domains *A1* through *A4* are out of registry with domains *B1* and *B2*. The unlabeled regions show a mixture of  $c(4 \times 2)$  and  $p(2 \times 2)$  surface reconstructions as well as defects and disordered (presumably unbuckled) regions. Antiphase boundaries

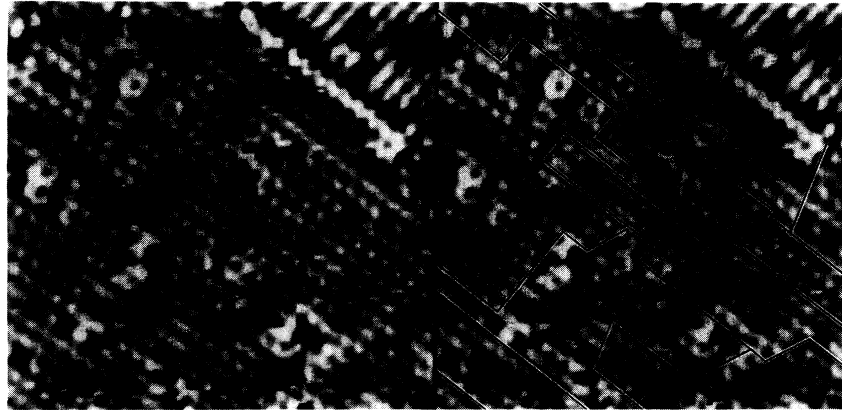


FIG. 3.  $200 \times 200 \text{ \AA}$  topograph of Si(001) taken at a temperature of 120 K at  $-2 \text{ V}$  sample bias and  $0.2 \text{ nA}$ . Domain boundaries have been marked at the right. Low-frequency components have been removed to cause the two terraces to appear at the same height.

[i.e.,  $p(2 \times 2)$  ordering] are observed between domains  $A2$  and  $B2$ ,  $B2$  and  $A1$ , and  $A1$  and  $B1$ . The upper right corner of the image shows a single atomic step down to another terrace. In the region shown, some of the rows are not buckled and appear as structureless bars.

Room-temperature images show buckled and symmetric appearing dimers; buckled dimers are found only in the vicinity of defects. These observations are consistent with either the symmetric or the asymmetric description of the dimer. Our low-temperature measurements allow us to discriminate between these models; we will show in the following discussion that our observation at 120 K of an increase in the number of buckled dimers, at the expense of symmetric appearing dimers, is consistent only with the asymmetric dimer description.

To help visualize the interplay of defect-induced strain and dimer-dimer coupling we present schematic potential energy plots in Fig. 4. The curves in Fig. 4(a) represent the symmetric dimer model. The solid line describes the unperturbed symmetric configuration, and the dashed curve depicts a normally symmetric dimer which, under the influence of a defect, is *forced* to buckle; in both cases the potential is *monostable*. The induced asymmetry is most pronounced for dimers adjacent to a defect; the next dimer in the row experiences an asymmetry which is smaller in magnitude, and of the opposite sense. Dimers further removed from the defect tend increasingly toward a symmetric configuration. This description of the dimers cannot accommodate the observed temperature-dependent growth of buckled-dimer domains. We note that buckling does not increase as a result of lattice strain varying in some way with temperature; defect-induced strain is essentially constant with temperature [24]. Within the symmetric dimer model, a dimer experiencing a defect-induced asymmetry would appear buckled whether at 120 K or room temperature. Increased thermal excitation could not mask asymmetry; the mean angle of tilt, as sensed by the STM, would not change.

The bistable asymmetric description of the dimer, depicted in Fig. 4(b), naturally leads to thermally activated behavior; indeed, a coupled system of bistable dimers has been predicted to display an order-disorder transition below room temperature [25–27]. Individual dimers will feel a preference for one direction of tilt [as shown by the dashed line in Fig. 4(b)] as a result of coupling to neighboring dimers. Below some critical temperature these interactions will cause the system to form long-range order; at room temperature, thermal excitations are sufficient to overcome the tendency to order and dimers rapidly switch orientation leading to a symmetric appearance in STM images. The presence of defects modifies this picture [28]. The defect-dimer interaction is similar to the dimer-dimer interaction in that it induces a preference for one tilt direction; however, it differs in one important regard; the buckling influence of a defect is static, with the result that dimers adjacent to defects appear pinned in one configuration, even at room temperature. With increasing distance from a defect, strain dissipates and the static asymmetry forced upon the dimers is reduced. Our present observations fit this picture very well; defects serve to pin nearby dimers into an ordered configuration at room temperature. At lower temperatures, it is apparent that domains nucleated at defects gradually ex-

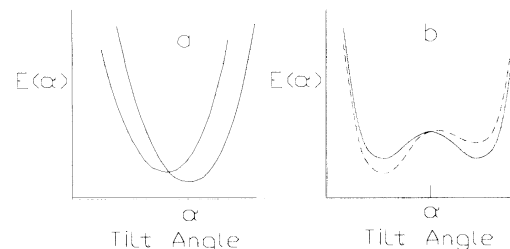


FIG. 4. Schematic potential energy plots for (a) the symmetric dimer model, and (b) the asymmetric dimer model.

tend. Defects have the effect of smearing out the transition to order over a wide temperature range; order is observed at room temperature where in the absence of defects none would be expected, and the extent to which long-range order develops at low temperature is limited when neighboring domains which are out of phase collide.

Finally, we note that it cannot be determined whether or not buckled dimers would be observed at 120 K in the absence of defects. It could be suggested that the patches of symmetric appearing dimers which persist at 120 K (such as in the central region of Fig. 2) result because  $T_c$  (of the defect free system) is lower than 120 K and only dimers sufficiently near to defects appear buckled. Alternately, it might be that 120 K is below  $T_c$  but these regions are frustrated by the out-of-phase influence of surrounding defects.

In conclusion, we have directly observed that on cooling to 120 K the number of buckled dimers increases at the expense of symmetric appearing dimers. This result has been discussed in terms of the symmetric and asymmetric dimer models. Symmetric dimers would not display the observed temperature-dependent growth of buckled-dimer domains. The asymmetric dimer description, however, naturally accounts for thermally activated behavior and we conclude that dimers on the Si(001) surface are asymmetric.

Helpful discussions with G. P. Kochanski, D. R. Hamann, J. E. Rowe, and F. H. Stillinger are gratefully acknowledged.

- 
- [1] R. E. Schlier and H. E. Farnsworth, *J. Chem. Phys.* **30**, 917 (1959).
  - [2] J. J. Lander and J. Morrison, *J. Chem. Phys.* **37**, 729 (1962).
  - [3] T. D. Poppendieck, T. C. Ngoc, and M. B. Webb, *Surf. Sci.* **75**, 287 (1978).
  - [4] M. J. Cardillo and G. E. Becker, *Phys. Rev. Lett.* **40**, 1148 (1978); *Phys. Rev. B* **21**, 1497 (1980).
  - [5] J. A. Appelbaum, G. A. Baraff, and D. R. Hamann, *Phys. Rev. Lett.* **35**, 729 (1975); *Phys. Rev. B* **11**, 3822 (1975); **12**, 5749 (1975); **14**, 588 (1976); **15**, 2408 (1977).
  - [6] G. P. Kerker, S. G. Louie, and M. L. Cohen, *Phys. Rev. B* **17**, 706 (1978).
  - [7] J. E. Rowe, *Phys. Lett.* **46A**, 400 (1974).
  - [8] S. Y. Tong and A. L. Maldondo, *Surf. Sci.* **78**, 459 (1978).
  - [9] D. J. Chadi, *Phys. Rev. Lett.* **43**, 43 (1979).

- [10] M. Aono, Y. Hou, C. Oshima, and Y. Ishizawa, *Phys. Rev. Lett.* **49**, 567 (1982).
- [11] I. Stensgaard, L. C. Feldman, and P. J. Silverman, *Surf. Sci.* **102**, 1 (1981).
- [12] R. M. Tromp, R. G. Smeenk, and F. W. Saris, *Phys. Rev. Lett.* **46**, 9392 (1981).
- [13] Y. Chabal, *Surf. Sci.* **168**, 594 (1986).
- [14] S. J. White, D. C. Frost, and K. A. R. Mitchell, *Solid State Commun.* **42**, 763 (1982).
- [15] W. S. Yang, F. Jona, and P. M. Marcus, *Phys. Rev. B* **28**, 2049 (1983).
- [16] R. M. Tromp, R. J. Hamers, and J. E. Demuth, *Phys. Rev. Lett.* **55**, 1303 (1985); R. J. Hamers, R. M. Tromp, and J. E. Demuth, *Phys. Rev. B* **34**, 5343 (1986).
- [17] E. Artacho and F. Yndurain, *Phys. Rev. Lett.* **62**, 2491 (1989).
- [18] G. K. Wertheim, D. M. Riffe, J. E. Rowe, and P. H. Citrin (unpublished).
- [19] K. C. Pandey, in *Proceedings of the Seventeenth International Conference on the Physics of Semiconductors*, edited by D. J. Chadi and W. A. Harrison (Springer, New York, 1985), p. 55.
- [20] M. C. Payne, N. Roberts, R. J. Needs, M. Needels, and J. D. Joannopoulos, *Surf. Sci.* **211**, 1 (1989).
- [21] N. Roberts and R. J. Needs, *Surf. Sci.* **236**, 112 (1990).
- [22] R. A. Wolkow (to be published).
- [23] R. J. Hamers and U. K. Kohler, *J. Vac. Sci. Technol. A* **7**, 2854 (1989).
- [24] Strain propagation could change significantly only if the force constants of the lattice were altered appreciably. This in turn would require that the change in excitation of lattice vibrations be sufficient for anharmonicity to come into play. Our temperature change clearly does not cause a significant change in excitation (the Debye temperature for silicon is 645 K) and the defect-induced strain field may be assumed constant over our temperature range.
- [25] J. Ihm, D. H. Lee, J. D. Joannopoulos, and J. J. Xiong, *Phys. Rev. Lett.* **51**, 1872 (1982).
- [26] T. Tabata, T. Aruga, and Y. Murata, *Surf. Sci.* **179**, L63 (1987).
- [27] G. P. Kochanski and J. E. Griffith, *Surf. Sci.* **249**, L293 (1991).
- [28] We cannot prepare a surface which is free of defects. In any case, step edges also cause buckling, so buckle inducing "defects" can never be eliminated. The most important point regarding the defect density observed in this work is that it is sufficiently low to allow us to observe that on cooling to 120 K, the number of buckled dimers clearly increases, at the expense of symmetric appearing dimers.

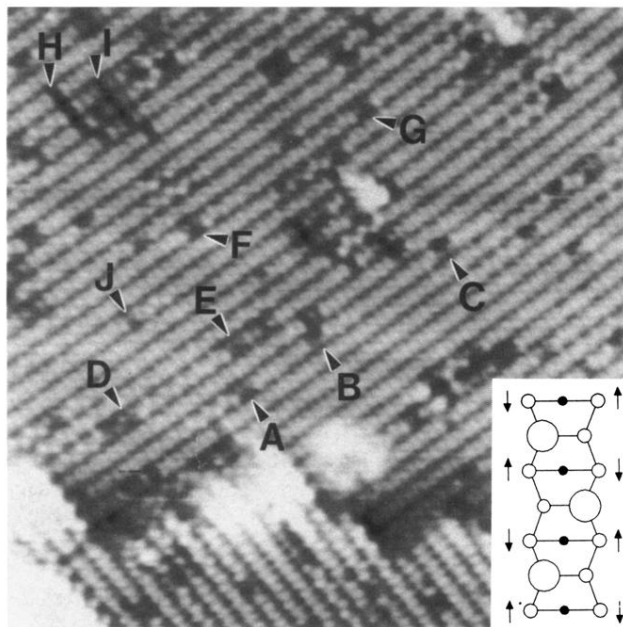


FIG. 1.  $240 \times 240 \text{ \AA}$  room-temperature constant-current topograph of Si(001) taken at  $-2 \text{ V}$  sample bias and  $0.3 \text{ nA}$ . Inset: A simple schematic view of the lattice strain which acts to couple adjacent dimers in an anticorrelated manner.

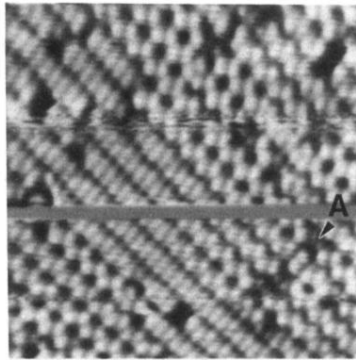


FIG. 2.  $110 \times 110 \text{ \AA}$  topograph of Si(001) taken at a temperature of 120 K at  $-2 \text{ V}$  sample bias and  $0.4 \text{ nA}$ . (The horizontal band resulted from an equipment malfunction during acquisition.)

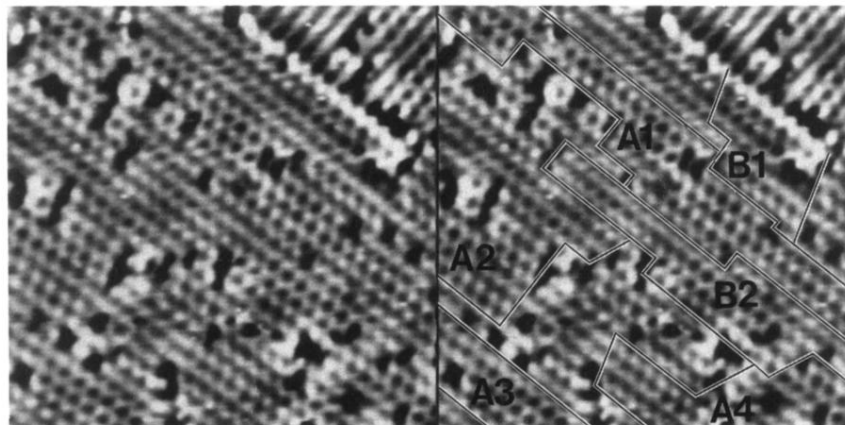


FIG. 3.  $200 \times 200 \text{ \AA}$  topograph of Si(001) taken at a temperature of 120 K at  $-2 \text{ V}$  sample bias and  $0.2 \text{ nA}$ . Domain boundaries have been marked at the right. Low-frequency components have been removed to cause the two terraces to appear at the same height.